AN IMPROVED APPROACH TO ESTIMATE WIND EROSION IN WASHINGTON'S COLUMBIA PLATEAU USING GOOGLE EARTH ENGINE

by

Jadey Nicole Ryan

A professional paper submitted in partial fulfillment
of the requirements for the degree

of

Master of Science

in

Land Resources and Environmental Sciences

MONTANA STATE UNIVERSITY
Bozeman, Montana

August 3, 2023

DEDICATION

To my family – Greg, Susan, Roger, Cheryl, Jeff, Jan, and Michael – who taught me the importance of education and "learning how to learn," and then supported me through my 11-year journey through higher education. To my husband, Matt, who constantly reminded me that I am capable of anything I set my mind to and always made sure I had food and treats to fuel my brain. To our trio of kittens, Mai, Tai, and Skye, who revitalized me with countless cuddle breaks.

ACKNOWLEDGEMENTS

Thank you to my supervisor and graduate committee member, Dr. Dani Gelardi, for supporting my professional and personal development, encouraging me when the learning curves became a little too steep, and modeling compassionate solutions-based thinking. I would also like to thank my colleagues at the Washington State Department of Agriculture Natural Resources Assessment Section for building my confidence as a scientist, especially Katie Noland, Jaclyn Hancock, and Leslie Michel.

I also would like to express my gratitude to my advisor, Dr. Scott Powell, for guiding me throughout my coursework and professional paper with sound advice about science never being done or perfect. Thank you to my other graduate committee members Dr. Bob Peterson and Dr. Tracy Sterling; the LRES program manager Marni Rolston; and every LRES instructor I've had the pleasure of learning from. I am grateful for the opportunity to pursue an online master's degree while working full-time.

TABLE OF CONTENTS

LIST OF TABLES

LIST OF FIGURES

LIST OF SUPPLEMENTARY TABLES

Supplementary Table Page

LIST OF SUPPLEMENTARY FIGURES

GLOSSARY OF ACRONYMS AND FACTORS

ARS: Agricultural Research Service

CC: Canopy Cover

COG: Combined Residue Factor

DEM: Digital Elevation Model

EF: Erodible Fraction

GEE: Google Earth Engine

GIS: Geographic Information Systems

GLDAS: Global Land Data Assimilation System

gSSURGO database: Gridded Soil Survey Geographic database

K': Soil Roughness Factor

K'_r: Topographic Roughness Factor

NASA: National Aeronautics and Space Administration

NDVI: Normalized Difference Vegetation Index

NOAA: National Oceanic and Atmospheric Administration

NRCS: Natural Resources Conservation Service

Q_{max}: Maximum Transport Capacity of Wind (kg/m)

RS: Remote Sensing

RTMA: Real-Time Mesoscale Analysis

RWEQ: Revised Wind Erosion Equation

s: Critical Field Length (m)

SCF: Soil Crust Fraction

SLR_c: Soil Loss Ratio Crop Canopy

USDA: United States Department of Agriculture

WEPS: Wind Erosion Prediction System

WF: Weather Factor

x: Distance from Non-erodible Upwind Edge of Field (m)

ABSTRACT

Loss of soil from erosion leads to declining agricultural productivity, pollution of water bodies, hazardous air quality, and many other detriments to human and environmental health. The agricultural community in Washington State identified soil erosion as a priority concern in the Columbia Plateau. To target specific areas for monitoring and reducing erosion, decision-makers must have access to regional soil loss estimates. The time-consuming, labor-intensive, and site-specific nature of conventional field measurements makes measuring soil erosion at the regional scale nearly impossible. Alternatively, geographic information systems (GIS), remote sensing (RS) datasets, and Google Earth Engine (GEE), a cloud-based geospatial analysis platform, can be used to estimate erosion at the regional scale. In this study, I implemented the Revised Wind Erosion Equation (RWEQ) model to assess wind-driven soil erosion using GEE. Combining a variety of geospatial and RS datasets, I generated monthly erosion estimates for the year 2018 with a spatial resolution of 0.25°. Erosion was lowest during the late fall through winter months, and highest during the summer months when precipitation was scarce and wind speeds were high. In this proof-of-concept study, some key parameters that influence spatiotemporal variability (i.e., tillage, irrigation, plant residue, and wind barriers) were simplified or omitted. The maximum erosion estimate, aggregated to the year, was consistent with results from another study (7.01 and 8.8 kg/m^2, respectively). Both values surpass the annual soil loss tolerance threshold established by the US Department of Agriculture (0.25 – 1.25 kg/m^2). This range defines the maximum rate of soil loss that can occur while sustaining crop productivity. The estimates from my study emphasize the importance of regional erosion estimates and control measures. My study demonstrates the feasibility of using GIS, RS, and GEE to automate and visualize regional erosion estimates. To encourage transparency, reproducibility, and community collaboration, my code is published in a public GitHub repository. Lastly, my study provides a framework for the future development of a decision-support tool to access and visualize erosion susceptibility in various time periods and regions. Decision-makers can leverage these accessible monthly erosion estimates to guide research and conservation efforts.

INTRODUCTION

Soil erosion poses a serious threat to global human, environmental, and economic health (Lal, 1998; Montanarella et al., 2016). Erosion occurs when wind, water, or human disturbance (i.e., agriculture, deforestation, urbanization) detaches, transports, and deposits soil particulates off-site (Pimentel et al., 1995). The consequential loss of fertile topsoil and increased dust emissions result in reduced agricultural productivity (Lal and Moldenhauer, 1987; Pimentel, 2006), increased sediment and contamination of waterbodies (Rickson, 2014; Uri, 2000), physical damage to infrastructure (Duniway et al., 2019), traffic fatalities due to low visibility (Figure 1) (Ashley et al., 2015), and hazardous air quality (Crooks et al., 2016; Joshi, 2021).

Figure 1. On March 28, 2021, a dust storm resulted in a seven-car pile-up involving minor injuries near Richland, WA. Photo from Washington State Patrol Trooper C. Thorson (Vaughn, 2022)

Arid and semiarid land with scarce vegetation and sand or sandy loam soils are particularly susceptible to wind-driven erosion (Fryrear et al., 1998; McGuire, 2011). In Washington's Columbia Plateau, for example, wind erosion and air quality have been a challenge since farming transformed the native shrub-steppe over 120 years ago (Saxton et al., 1999). Agriculture in the Columbia Plateau generates over $3 billion annually, and is critical for global food security and Washington rural livelihoods (Saxton et al., 1999; WSDA, 2021).While conservation efforts have made some improvements in the region, a recent stakeholder engagement process identified wind erosion as a continued major soil management challenge (Hills and Benedict, 2021).

Approaches to Estimating Wind Erosion

To effectively identify and manage wind erosion, a better understanding of natural and anthropogenic erosion processes, their interactions, and predictions of the resulting soil loss are essential (Poesen, 2018). Measuring the transport of eroded soil particles and dust emissions in the field requires complex equipment, analytical methods, and technical expertise (Fryrear et al., 1991). Advances in geographic information systems (GIS) and remote sensing (RS) technologies make it possible to scale from field observations to regionally model wind erosion and its spatial patterns and drivers (Borrelli et al., 2017; Yang et al., 2022). These technologies use a different suite of equipment, methods, and expertise to generate erosion estimates that can later be validated using field measurements.

Many wind erosion models exist with varying degrees of complexity and applicability (Jarrah et al., 2020). The Revised Wind Equation (RWEQ) model was developed to improve upon its predecessor, the Wind Erosion Equation (Woodruff and Siddoway, 1965). RWEQ modifies previous parameters based on weather inputs and adds new parameters not previously considered (Fryrear et al., 1998, 2000). Validated with field erosion data from 45 site years, the predominantly empirical RWEQ model became widely used (Jarrah et al., 2020). However, the RWEQ often underestimated erosion and required calibration to the local climate to accommodate deviations from the average condition (Fryrear et al., 2000; Jarrah et al., 2020). Average conditions are simulated based on historical statistics, as described in Skidmore and Tatarko (1990). In response, the Agricultural Research Service (ARS) of the US Department of Agriculture (USDA) developed a more process-based model called the Wind Erosion Prediction System (WEPS) (Wagner, 2013). WEPS simulates hydrology, plant growth and decomposition, and soil surface erodibility, while considering user inputs of site-specific climate, soil type, and land management (Tatarko et al., 2019). Additionally, WEPS provides estimates of soil loss, saltation, suspension, and PM_{10} emissions (particulates <10 μm in aerodynamic equivalent diameter) (Jarrah et al., 2020). The advanced technology of WEPS requires higher data inputs and technical expertise than the RWEQ, resulting in a tradeoff between ease-of-use and accuracy. For a more detailed comparison of these models, see Supplementary Table 1.

The Columbia Plateau PM_{10} Project was initially funded in 1993 by the US Environmental Protection Agency and Washington State Department of Ecology to 1) predict and measure PM_{10} emissions and 2) develop and promote farming practices to control wind erosion (Chung et al., 2011). Scientists from the Washington State University, USDA ARS, and University of Idaho later became collaborators in the multi-disciplinary team who measured erosion in agricultural fields and wind tunnels, or estimated erosion using GIS and RS (Kjelgaard and Chandler, 2004; Sharratt and Schillinger, 2005; G. Feng and Sharratt, 2007; G Feng and

Sharratt, 2007; Feng and Sharratt, 2009; Gao et al., 2013; Sharratt et al., 2015; Pi et al., 2017, 2020).

This research from the Columbia Plateau PM_{10} Project emphasizes the need for field measurements and quality high spatiotemporal resolution data for accurate, validated erosion estimates. Additionally, these studies identified barriers to generating reliable model outputs when scaling from field to region. The following section summarizes four requirements for GIS and RS applications in regional erosion models: 1) quality input data, 2) big data storage and computing resources, 3) calibration, and 4) validation.

Requirements for GIS and RS Applications in Large Scale Erosion Models

1. Quality Input Data

Drivers of erosion (i.e., surface vegetation, soil properties, weather, tillage) change in space and time. To accurately estimate erosion, models require valid field measurements of these factors at the relevant spatial and temporal resolution. Without high spatiotemporal resolution data, it is nearly impossible to scale accurate process data from fields to regions. Many studies have tested the validity and feasibility of modeling erosion with GIS and RS (Borrelli et al., 2018; El Jazouli et al., 2017; Flanagan et al., 2007; Hu et al., 2015; Pandey et al., 2007; Polykretis et al., 2020; Shirriff et al., 2022; Vrieling, 2006; Zhang et al., 2022; Zobeck et al., 2000). For example, the European Union modified their use of an erosion model [Revised Universal Soil Loss Equation (Renard et al., 1996)] to the continental scale by updating the input factors to use high spatiotemporal resolution RS data (Panagos et al., 2015).

2. Big Data Storage and Computing Resources

Upscaling wind erosion models from fields to regions with GIS and RS requires large amounts of data storage and computing resources. Borrelli et al. (2017) used the RWEQ to model wind erosion across arable land in the European Union from 2001 to 2009 with three different GIS environments and a series of R and Python scripts. With several terabytes of data storage and muti-tasking calculations on a designated server, the calculations took 25 days to obtain the final results (Borrelli et al., 2017). Alternatively, the Google Earth Engine (GEE) platform offers cloud computing capabilities with a multi-petabyte catalog of geospatial data (Gorelick et al., 2017). The data catalog contains more than 40 years of satellite imagery, climate reanalysis datasets, and other geospatial data, thereby allowing access to these data without needing to download and store them locally (Gorelick et al., 2017). Recent studies have implemented various soil erosion models with GEE (Elnashar et al., 2021; Kumar et al., 2022; Wang et al., 2020; Zhang et al., 2022).

3. Calibration

Erosion models often lack adequate calibration, testing, and uncertainty assessment (Batista et al., 2019). Batista et al. (2019) found that the small percentage of model evaluation studies often demonstrated 1) the limited predictive accuracy of uncalibrated models, 2) that soil erosion measurements are highly variable and poorly understood, 3) the quality of spatial predictions are dubious, and 4) that model outputs are full of uncertainties. In ‘blind’ evaluations, models were parameterized using values from the literature, run, and then tested against the observations (Batista et al., 2019). Conversely, calibrated models were trained using field or sensor collected soil, plant, and rainfall data to minimize prediction error (Batista et al., 2019).

The calibration process involved adjusting parameters to bring the predicted values within range of the observed values. Many other researchers agree with the stance in Batista et al. (2019) that the predictive accuracy depends on the quality of the model calibration, due to the inherent spatial and temporal variability in erosion processes (Evans and Brazier, 2005; Jetten et al., 2003; Mahmoodabadi and Cerdà, 2013; Stroosnijder, 2005).

4. Validation

Similar to calibration requirements, many argue that field-based assessments are necessary to validate modelled erosion estimates (Batista et al., 2019; Evans and Brazier, 2005; Nearing, 2000; Vrieling, 2006). For example, Fischer et al. (2017) modeled erosion in southeastern Germany using the Universal Soil Loss Equation with inputs from high-resolution (1-m to 5-m) RS and geospatial data. They also visually classified the degree of erosion damage from orthorectified aerial photos of 8,100 fields after erosive events (Fischer et al., 2018). Predicted soil loss from the model was significantly correlated with the visual soil loss classes, supporting the validity of both methods (Fischer et al., 2018). Success of these methods required highly resolved geospatial data and highly trained personnel to accurately interpret the extent of erosion damage in the aerial photos.

Problem Statement

The Columbia Plateau is valuable land for human and animal populations, agricultural productivity, and hydrological processes via the Columbia and Snake Rivers. Erosion and its associated loss of fertile topsoil, increased dust emissions, water quality degradation, and air quality contamination threaten the well-being of the region's inhabitants and the economic value of the land. Erosion prevention and mitigation is especially urgent, as it may take 10 to 20 years to replace a quarter-inch layer of lost topsoil (McGuire, 2011). For decision-makers to prioritize limited funds and target conservation efforts, they must have access to accurately modeled erosion estimates.

The Columbia Plateau PM_{10} Project validated the use and applicability of several erosion models. However, funding was eliminated in 2011, effectively dissolving the project team and faltering the efforts to regionally quantify wind erosion. Most project studies incorporated either spatially or temporally robust inputs, but not both. For example, Feng and Sharratt (2007) used static 40-year average annual precipitation data in the WEPS model to simulate erosion across Adams County. In another example, Pi et al. (2017) measured weather, soil loss, vegetation, and soil properties in one field during 12 wind events over four years. They reprogrammed the RWEQ model with Microsoft Excel, simulated soil loss, and then tested model performance using their field measurements (Pi et al., 2017). The first example resulted in a spatial distribution of erosion estimates using outdated weather inputs, while the second example provided a temporal distribution of erosion at a single point in one field. For model predictions to accurately inform erosion field research and mitigation, both spatial and temporal data must be current and high resolution.

Additionally, the workflow of accessing quality input data, computing model inputs and outputs, and visualizing the results must be improved. Many studies described a manual process of downloading data from databases and implementing the model in Excel or a GIS environment. These workflows do not easily scale to larger time periods or regions, nor do they comply with FAIR (Findable, Accessible, Interoperable, Reusable) principles of scientific data management and stewardship (Wilkinson et al., 2016). Some manuscripts included a statement that data or tools would be shared upon request. In my experience, and in the studies described in Watson (2022), researchers either ignore or decline these requests. This behavior reduces the transparency and reproducibility of their work.

While modeling is necessary for identifying areas with high erosion susceptibility, the outputs are generally locked in paywalled manuscripts that are not accessible or actionable to decision-makers. Instead, erosion estimates must be presented in publicly available decision-support tools that land managers and policymakers can access when prioritizing limited funds, identifying areas for additional research, and targeting conservation incentives in specific regions. The Daily Erosion Project is one example of a tool that presents daily water erosion estimates in multiple Midwest states within an interactive web map (Gelder et al., 2018).

Study Objectives

As the first step in a multiphase strategy to measure and reduce erosion in Washington, my study aimed to improve an existing workflow for modeling wind erosion with the RWEQ in two ways:

1) Instead of using outdated weather inputs, I integrated high-resolution gridded climate datasets that assimilate near-real time conventional and satellite-derived observations. However, to narrow the scope of my project, I simplified or omitted other key spatiotemporal parameters (i.e., tillage, plant residues). This study provides a proof-of-concept for replacing static, empirical climate inputs with dynamic data sources.
2) I used the GEE platform for its expansive data catalog, multi-petabyte storage, computational power, and programming capabilities. GEE allowed me to estimate monthly erosion across

the Columbia Plateau at 0.25° spatial resolution for the year 2018. Programming the calculations increases the automation of the workflow. Additionally, the scripts can easily be modified to estimate erosion for different regions and time periods. For transparency and reproducibility, I published the code in a public GitHub repository.

I validated this approach by comparing my results with those from a study in the same region and time period (Pi et al., 2020). My study serves as a framework for the future development of a decision-support tool to access and visualize erosion susceptibility in various time periods and regions.

MATERIALS AND METHODS

Study Area

Located in the lowland between the Okanogan Highlands on the north, Cascade Mountains on the west, Rocky Mountains on the east, and Blue Mountains on the south, the Columbia Plateau spans about 75,000 km^2 across Washington, Oregon, and Idaho. This study focuses on nearly 57,000 km^2 in Washington. Within the plateau is its smaller irrigated counterpart, the Columbia Basin. Deposits from glacial floods, basalt lava flows, and wind-driven loess formed the steep river canyons, tall ridges, and expansive plateaus that characterize this region (DNR, 2021). The Cascades cast a rain shadow over the basin, resulting in a semi-arid climate with hot, dry summers and cold winters, with generally between 100 and 500 mm of annual precipitation (Saxton et al., 1999; WSU, 2023). Precipitation decreases from west to east, and native vegetation shifts from sagebrush-steppe in the west to meadow-steppe in the east (Sharratt and Schillinger, 2005). These patterns result in a soil gradient of low organic matter sands to high organic matter silt loams from west to east (Sharratt and Schillinger, 2005). Sand and sandy loam soils are most prone to wind erosion, resulting in the loss of valuable clay, silt, and organic matter in the topsoil (McGuire, 2011). The Columbia Plateau supports almost 28,000 km^2 of livestock grazing, irrigated cropland, and rain-fed agricultural production (Figure 2). More than half (15,000 km^2) of this agricultural land is not irrigated and uses a crop rotation of winter wheat every other year and summer fallow between crop years (i.e., Cereal Grain in Figure 2) (WSDA, 2023). This land use often leaves the soil bare and vulnerable to erosion (Schillinger and Papendick, 2008). The topography, climate, vegetation, soil properties, and overall land management within the Columbia Plateau make this region particularly susceptible to erosion.

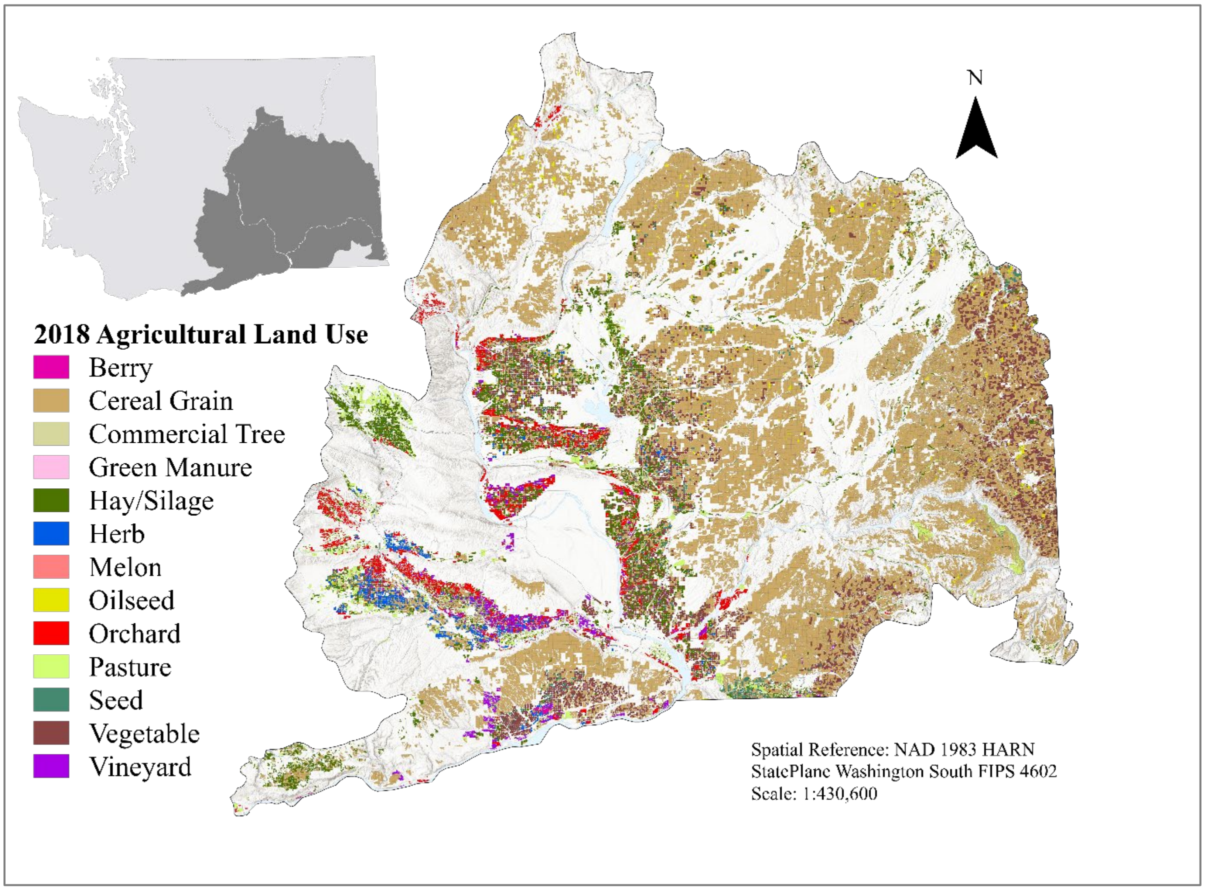

Figure 2. Agricultural land use (28,000 km^2) within the Columbia Plateau (57,000 km^2) in Washington State. More than half (15,000 km^2) of this is Cereal Grain, which is not irrigated and is in fallow every other year, leaving the soil susceptible to erosion (Schillinger and Papendick, 2008; WSDA, 2023)

Revised Wind Erosion Equation

Fryrear et al. (1998) developed the RWEQ model to improve on the previous Wind Erosion Equation (Woodruff and Siddoway, 1965) by requiring additional information about the agricultural fields being modelled. As an empirical model, the RWEQ was developed and validated with field erosion data from 45 site years, considering weather, soil, vegetation, field management, and topography (Fryrear et al., 2000). RWEQ's basic premise follows Newton's First Law of Motion (Fryrear et al., 2000). When the wind force exceeds the resisting forces that help anchor the soil in place (i.e., surface roughness, soil wetness, soil erodible fraction, vegetative cover), then wind-driven soil erosion occurs (Fryrear et al., 2000). I briefly mention many assumptions and simplifications within these equations. In the Errors and Assumptions section, I elaborate on their implications and suggest new data sources or methods to be used in the next phase of this project.

The RWEQ estimates the potential soil loss (PSL) as

$$PSL = \frac{2x}{s^2} Q_{max} e^{-\left(\frac{x}{s}\right)^2}, \qquad (Eq. 1)$$

where *PSL* is the potential soil loss (kg/m^2); Q_{max} is the maximum transport capacity (kg/m) (Eq. 2); x is the distance from the non-erodible upwind edge of the field (m); and s is the critical field length (m) (Eq. 3) (Fryrear et al., 2000).

Most studies did not explain how x was calculated or provide the range of x values parameterized in their models. Fryrear et al. (1991) presented a range of x values from a field experiment in Big Spring, TX from 0 m to 200 m. Wang et al. (2020) set x to a constant value (55 m), with no explanation of how they arrived at that value. Without guidance from the literature on how to derive x, I somewhat arbitrarily set x to 150 m in this equation. Additional thoughts on how to dynamically calculate x are presented in the Errors and Assumptions section.

In Fryrear et al. (2000), Q_{max} and s are calculated as

$$Q_{max} = 109.8 \times WF \times EF \times SCF \times K' \times COG \qquad (Eq. 2)$$

$$s = 150.71 \times (WF \times EF \times SCF \times K' \times COG\,)^{-0.3711} \qquad (Eq. 3)$$

where *WF* is the weather factor (kg/m) (Eq. 4); *EF* is the erodible fraction (dimensionless) (Eq. 6); *SCF* is the soil crust factor (dimensionless) (Eq. 7); *K'* is the soil roughness factor (dimensionless) (Eq. 8); and *COG* is the combined residue factor (dimensionless) (Eq. 9).

The weather factor (WF) is generally the most significant factor affecting wind erosion, as it contains the wind parameters that drive the detachment and movement of soil particles (Fryrear et al., 1991). WF was calculated as

$$WF = \frac{\sum_{i=1}^{N} U_2(U_2 - U_t)^2 \times N_d \times \rho}{N \times g} \times SW \times SD\,, \qquad (Eq. 4)$$

where U_2 is the wind speed at 2 m (m/s); U_t is the threshold wind speed at 2 m (assumed 5 m/s); N is the number of wind speed observations in the month; N_d is the number of days in the month; ρ is the air density (kg/m^3); *g* is acceleration due to gravity (m/s^2); *SW* is soil wetness (dimensionless) (Eq. 5); and *SD* is the snow cover factor (Fryrear et al., 2000). The threshold wind speed varies based on the soil and weather conditions; however, there are not yet reliable methods to calculate the threshold (Fryrear et al., 2000). Therefore, RWEQ assumes the threshold is 5 m/s, as supported by field measurements (Fryrear et al., 1991). When there is at least 25.4 mm (1 in) of snow, the snow factor is set to zero as wind erosion is assumed to be controlled (Fryrear et al., 2000).

Soil moisture reduces wind erosion by acting as a resisting force to the wind force that detaches and transports soil particles (Fryrear et al., 2000). However, too much soil wetness may lead to water erosion, which is not considered in this study. When the soil moisture from rain or irrigation has evaporated from sufficient solar radiation, the soil wetness factor is zero. Conversely, the factor is one when there is no rain. SW was calculated as

$$SW = \frac{ET - \left(R \times \left(\frac{R_d}{N_d}\right)\right)}{ET}, \qquad (Eq. 5)$$

where *ET* is potential relative evapotranspiration (mm); *R* is rainfall and irrigation (mm); R_d is the number of days there was rainfall; and N_d is the number of days in the period (Fryrear et al., 2000). To simplify this study, I omitted irrigation inputs because more than half of the study area is rainfed-only dryland. I will identify data sources for quantifying daily irrigation inputs in future work of this project.

RWEQ uses physical and chemical soil properties such as texture, organic matter, and calcium carbonate to estimate what fraction of the soil surface is erodible (Fryrear et al., 2000). Similarly, clay and organic matter help estimate the extent of soil aggregates breaking down and forming a crust (Fryrear et al., 2000). EF and SCF were calculated as

$$EF = \frac{29.09 + 0.31\,Sa + 0.17\,Si + 0.33\frac{Sa}{Cl} - 2.59\,OM - 0.95\,CaCO_3}{100}, \qquad (Eq. 6)$$

$$SCF = \frac{1}{[1 + 0.0066(Cl)^2 + 0.21(OM)^2]}, \qquad (Eq. 7)$$

where *Sa* is sand content (%); *Si* is silt content (%); *Sa/Cl* is the sand to clay ratio (%); *OM* is organic matter (%); $CaCO_3$ is calcium carbonate (%); and *Cl* is clay content (%) (Fryrear et al., 2000).

The soil roughness factor (*K'*) considers how tillage operations affect the soil surface conditions (i.e., surface crust, ridges and furrows, roughness, clod size), in addition to topography (Fryrear et al., 2000). Since spatial data sources for tillage operations do not yet exist in Washington, I simplified *K'* to consider only topographic roughness (K'_r) according to Wang et al. (2020) and Zhang et al. (2022) as

$$K'_r = \cos\alpha\,, \qquad (Eq. 8)$$

where α is the slope gradient (degrees). I used the built-in GEE 4-connected neighbours algorithm to calculate slope gradient from elevation (m).

COG, identified in Eq. 2 and 3, includes three different crop residue factors (Fryrear et al., 2000). One of these factors is the influence of growing crop canopies (SLR_c) on erodibility. SLRc was validated by Borelli et al. (2017) as an alternative to COG for equations 2 and 3

$$SLR_c = e^{-5.614\left(CC^{0.7366}\right)}, \qquad (Eq. 9)$$

where *CC* is canopy cover. I used the normalized vegetation difference index (NDVI) as a proxy for *CC*, justified by the linear relationship between NDVI and CC (Trout et al., 2008).

Data Acquisition and Processing

Using the GEE catalog, I imported the following weather data: the National Oceanic and Atmospheric Administration (NOAA) Real-Time Mesoscale Analysis (RTMA) dataset (Pondeca et al., 2011) and the National Aeronautics and Space Administration (NASA) Global Land Data Assimilation System (GLDAS) V2.1 dataset (Beaudoing et al., 2020). I also downloaded and imported a 10-meter resolution raster of air density from the Global Wind Atlas V3 (Davis et al., 2019). These three datasets provided the inputs to calculate WF.

I calculated K_r from the slope gradient, derived from the 10-meter resolution Digital Elevation Model from the U.S. Geological Survey 3D Elevation Program dataset in GEE (USGS, 2020).

COG was derived from the NDVI, which I accessed from the NASA MOD13Q1 V6.1 dataset in the GEE catalog (Didan, 2021). I selected pixels with the quality assurance summary band of 0, indicating the highest quality. Using the detailed quality assurance bitmask, I masked the pixels associated with water or clouds.

To calculate EF and SCF, I downloaded the relevant soil properties using R 4.3.0 (R Core Team, 2023) and the 'soilDB' R package (Beaudette et al., 2023), which provides an interface to the USDA Natural Resources Conservation Service (NRCS) Gridded Soil Survey Geographic (gSSURGO) database (Soil Survey Staff, 2023). After extracting the data, I used the R packages 'dplyr' (Wickham et al., 2023) and 'terra' (Hijmans et al., 2023) to process the gSSURGO data into a single raster for the entire study area. The raster contained a band for each soil property, in addition to the calculated erodible fraction and soil crust factors. The R script for this workflow can be found at https://github.com/jadeynryan/erosion/blob/main/R/soils.R. I then imported this raster into GEE to continue the computations with the other input factors.

All GEE JavaScript code can be accessed at https://github.com/jadeynryan/erosion/blob/main/js/soil_loss.js. I extracted twelve parameters from six data sources using either GEE or soilDB, which I then used to calculate the inputs for the RWEQ (Figure 3). I averaged the temporally dynamic parameters (SD, SW, and NDVI) to the monthly scale prior to calculating WF and SLRc. After calculating monthly PSL, I summed all the months to calculate the annual PSL. To map the input factors and the PSL, I exported the rasters as TIF files to Google Drive, imported them into R with the 'googledrive' package (McGowan and Bryan, 2023), and plotted them with the 'terra' package (Hijmans et al., 2023).

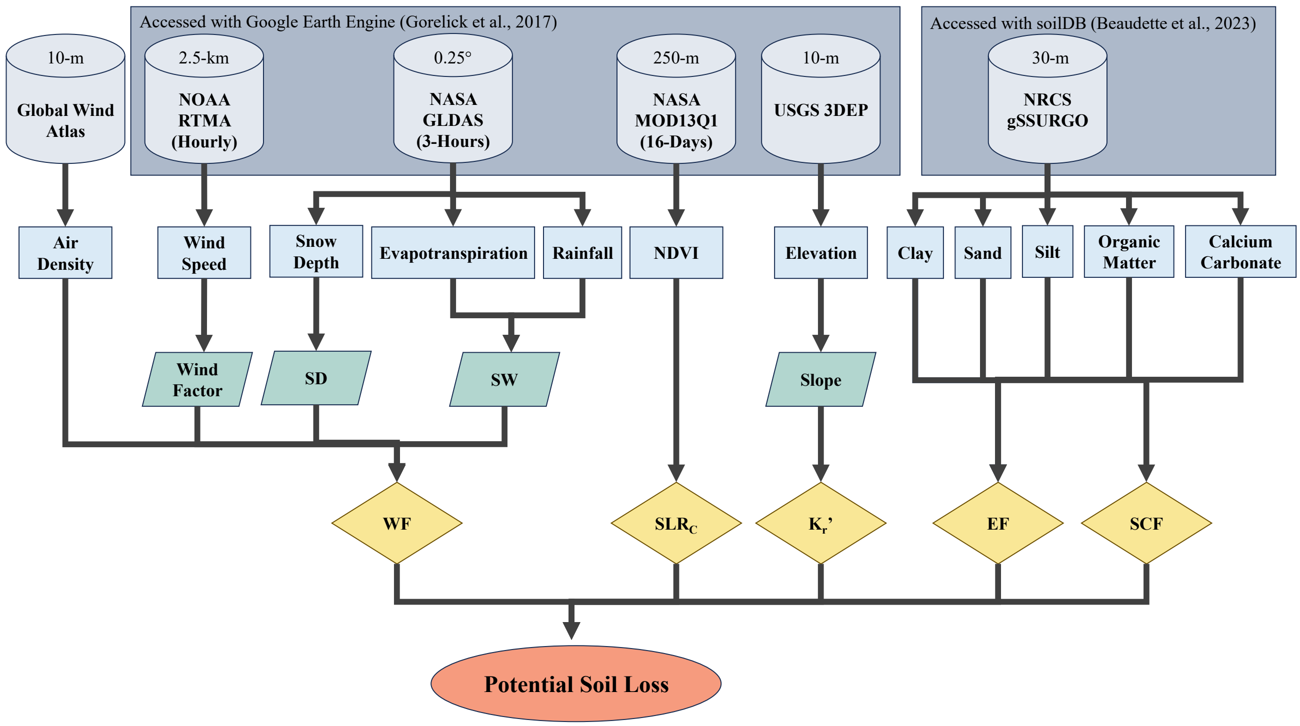

Figure 3. Workflow of data sources (cylinder), parameters (rectangle), calculated inputs (rhombus), and Revised Wind Erosion Equation input factors (diamond). ***WF***: weather factor; ***SLR$_c$***: influence of growing crop canopies on erodibility; ***K$_r$'***: topographic roughness factor; ***EF***: erodible fraction of soil; ***SCF***: soil crust factor

Model Estimate Validation

Although Pi et al. (2017) used the same RWEQ model as my study, the temporal data ranged from 2003 to 2006. My implementation of the RWEQ model uses the NOAA RTMA weather dataset that ranges from 2011 to near real-time (Pondeca et al., 2011). Therefore, I could only model erosion from 2011 onward and could not compare my results with those from Pi et al. (2017).

Alternatively, I compared my results with those from Pi et al. (2020) who used the WEPS model to estimate erosion from 2009 to 2018 in the same study area. Pi et al. (2020) obtained select current weather inputs (temperature, solar radiation, precipitation) from a network of meteorological stations in the region. Daily precipitation duration and time to peak were simulated using a climate generator model based on historic weather records (Pi et al., 2020). With the mixture of measured and simulated weather and climate data used in their study, it would have been interesting to compare the potential impacts on the PSL between our studies. However, monthly results in Pi et al. (2020) included the meteorological parameters and PSL aggregated across all years in their study. Therefore, I could only compare our annual estimates for the year 2018. To calculate annual PSL, I summed all monthly PSL estimates. I plotted their PSL estimates on top of my study's annual PSL raster for a qualitative spatial comparison. I then calculated the difference between our estimates for a quantitative comparison.

RESULTS AND DISCUSSION

Spatial and Temporal Variation

Monthly mean PSL estimates ranged from 0 kg/m^2 in January and December to 0.33 kg/m^2 in September (Figure 4). Across all months, the mean was 0.18 kg/m^2 and the median was 0.02 kg/m^2. The highest PSL estimates occurred in August and September with upper quartiles of 0.62 kg/m^2 and 0.68 kg/m^2, respectively. Throughout the late summer to early fall, the Columbia Plateau experiences high temperatures and scarce precipitation, resulting in low soil wetness and higher susceptibility to soil detachment and transport. If tillage and plant residues were considered in my study, PSL could have been higher in the spring months due to the baring of the soil in preparation for planting. PSL was lowest during the winter months (November – January) when increased soil wetness or snow cover weighed the soil down, reducing the amount of soil that the wind can transport.

The distribution of monthly PSL is skewed to the right, as shown by the consistently greater mean than median in Figure 4 and the ‘tail’ on the right side of the distribution in each histogram (excluding January and December) in Supplementary Figure 1. In every month, the bulk of the PSL estimates were 0 kg/m^2. However, from April through September, there were nearly as many high PSL estimates (> 0 kg/m^2) as low PSL estimates (0 to 0.1 kg/m^2), shown by the subtle U-shape in the histograms (Supplementary Figure 1).

Since my study focused on improving the climate and weather data inputs, while simplifying or omitting other key parameters (i.e., tillage and plant residues), these results should be interpreted with caution.

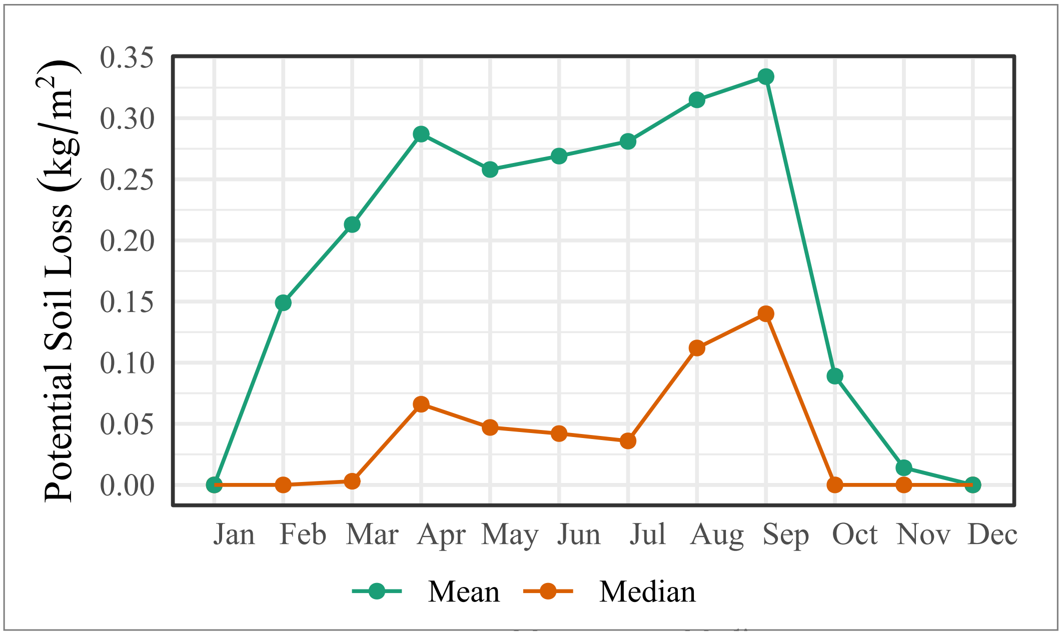

Figure 4. Monthly mean and median potential soil loss (kg/m^2) across all pixels in the Columbia Plateau study area in 2018

PSL estimates mostly remained spatially consistent from February through September (Figure 5). Areas with the highest estimates were in the central to eastern part of the Columbia Plateau, which is consistent with the dryland production systems (Figure 2) that have scarce precipitation, minimal green vegetation, and are most susceptible to erosion. There also appear to be erosion 'hotspots' in irrigated agricultural lands near the Snake and Columbia Rivers. However, this may not be the case once irrigation inputs are incorporated into the SW factor in a future iteration of this study.

Interestingly, something causes the erosion 'hotspots' to spatially invert from April to May, and then return to the same general spatial pattern in June. Visually assessing the maps of each input factor (see Figures in Supplementary Materials), I do not see an obvious explanation for this temporary change. I speculate that this may be a result of not considering land management in this model, as that area likely would have higher PSL in March and April as plant residues are tilled in the spring to expose bare soil for planting. The impact on wind erosion is two-fold: the plant residues no longer hold the soil in place and the soil is broken up, making it easier for wind to transport it.

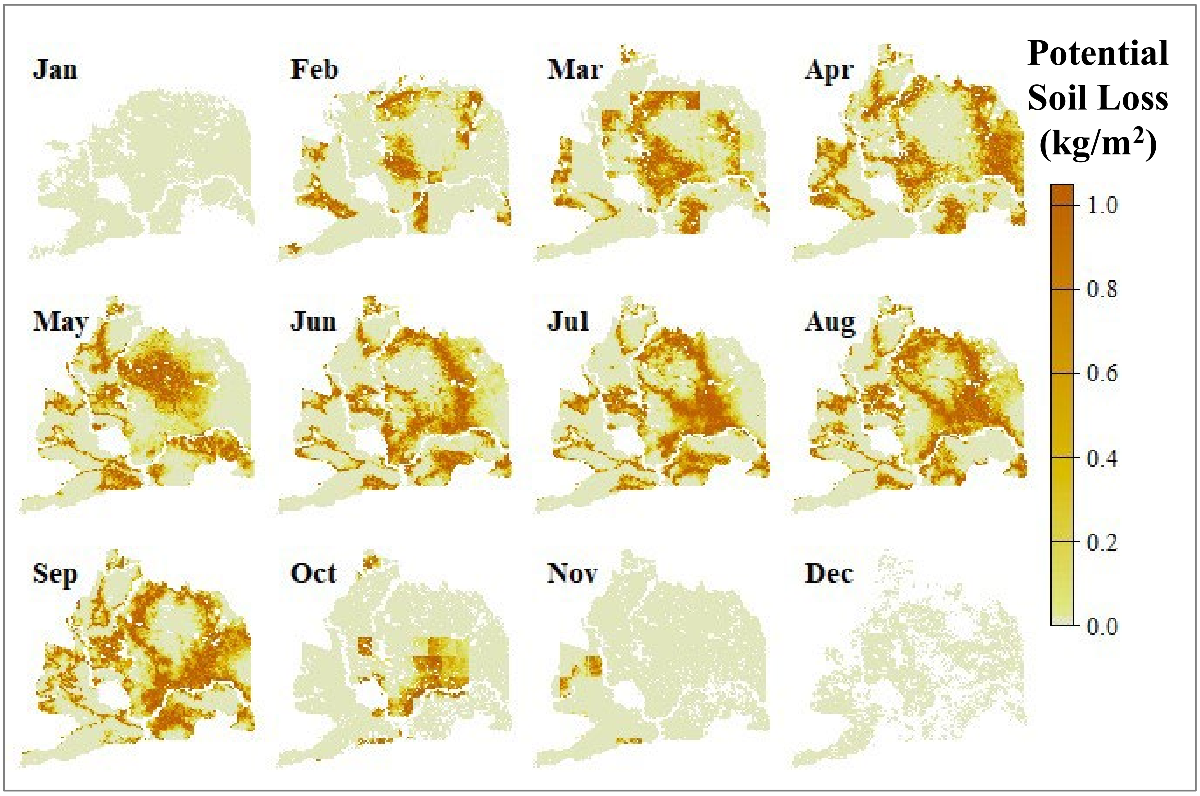

Figure 5. Spatiotemporal distribution of wind-driven potential soil loss (kg/m^2) at 0.25° spatial resolution each month of 2018

The areas with missing values resulted from non-soil surfaces (bedrock, water, etc.), lack of soil survey data in the Yakama Indian Reservation, and masked pixels from poor quality satellite imagery. This was especially apparent in January, February, and December when cloud cover was highest.

Comparison of Model Estimates

I evaluated the results of my RWEQ modeling exercise by comparing them to results from a peer-reviewed study in the same region that used the WEPS model (Pi et al., 2020). A subset of their annual PSL estimates for 2018 are plotted on top of the annual PSL raster generated in my study (Figure 6). The minimum PSL estimate in 2018 was 0 kg/m^2 in both modelling exercises. The maximum PSL estimate using WEPS was 8.8 kg/m^2, comparable to my 7.01 kg/m^2 maximum estimate using RWEQ. The overall means were 1.53 kg/m^2 (WEPS) and 1.99 kg/m^2 (RWEQ). Spatially, most zero-value WEPS points seem to align with either zero or low estimates on the RWEQ raster, though the locations of the maximums did not agree. The maximum PSL according to my RWEQ implementation occurred above the Snake River, whereas the maximum PSL modeled by WEPS occurred above the Columbia River.

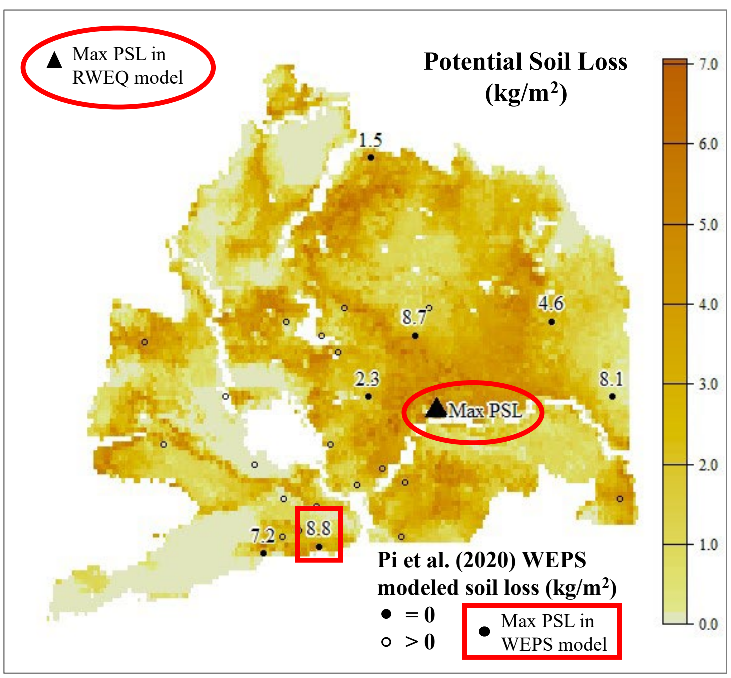

Figure 6. 2018 PSL (kg/m^2) estimates from the RWEQ model at 0.25° spatial resolution, with WEPS model point estimates (Pi et al., 2020) plotted on top. The maximum values are highlighted with the red circle (RWEQ) and rectangle (WEPS).

Table 1. Comparison of 2018 annual soil loss with Pi et al. (2020)

WSU AgWeatherNet Station[a]	Latitude	Longitude	2018 Annual Soil Loss (kg/m^2)		
			WEPS[b]	RWEQ[c]	Difference (RWEQ – WEPS)
McNary	45.97	-119.25	8.8	0.4	-8.4
Pullman	46.70	-117.15	8.1	0.8	-7.3
Paterson West	45.93	-119.65	7.2	0.9	-6.3
Lind	47.00	-118.57	8.7	4.9	-3.8
St. John	47.07	-117.58	4.6	1.5	-3.1
Connell Bench	46.70	-118.90	2.3	1.8	-0.5
McClure	46.37	-119.72	0.0	0.0	0.0
Triple-S	46.20	-119.50	0.0	0.1	0.1
Badger Canyon	46.17	-119.27	0.0	0.1	0.1
Konnowac Pass	46.47	-120.37	0.0	0.2	0.2
Ritzville	47.13	-118.47	0.0	0.6	0.6
Mae	47.07	-119.48	0.0	0.6	0.6
Smith Canyon East	46.27	-118.98	0.0	1.0	1.0
Wheeler	47.13	-119.07	0.0	1.6	1.6
Ringold	46.47	-119.17	0.0	2.0	2.0
Wheelhouse	46.02	-119.52	0.0	2.1	2.1
Station 4	46.05	-119.40	0.0	2.3	2.3
Hatton	46.78	-118.85	0.0	2.3	2.3
Almira	47.87	-118.88	1.5	3.8	2.3
Warden Golf	46.92	-119.12	0.0	2.6	2.6
Touchet	46.02	-118.67	0.0	3.1	3.1
K2H	46.28	-118.63	0.0	3.8	3.8
PK_McClenny	46.35	-118.80	0.0	3.8	3.8
Anatone	46.20	-117.10	0.0	4.5	4.5
Broadview	46.97	-120.50	0.0	5.0	5.0
Desert Aire	46.70	-119.92	0.0	NA	NA
Moses Lake	47.00	-119.23	0.0	NA	NA

[a] Pi et al. (2020) collected climate and weather data from these meteorological stations (https://weather.wsu.edu/)
[b] Annual soil loss as modeled by WEPS for 2018 by Pi et al. (2020)
[c] Annual soil loss as modeled by RWEQ in my study

While overall 2018 mean, minimum, and maximum estimates from each model agreed, results varied widely by geography. By location, RWEQ seemed to underestimate PSL compared to the highest estimates with WEPS (difference of -0.5 kg/m^2 to -8.4 kg/m^2) (Table 1). By frequency, many of the PSL estimates were overestimated by RWEQ compared to WEPS.

Annual Soil Loss Tolerances

USDA NRCS established soil loss tolerances, called T factors, for on-farm conservation planning (Schertz and Nearing, 2006). T factors represent the maximum annual soil loss that can occur while sustaining crop production (Schertz and Nearing, 2006). gSSURGO provides T factors in units of tons/acre/year. After unit conversion, soil loss tolerance ranged from 0.25 to 1.25 kg/m^2 (Figure 7). The majority of annual PSL estimates in my study exceeded the T factor (Figure 6, Figure 7). The mean annual PSL of 1.99 kg/m^2 exceeds even the most tolerant T factor (1.25 kg/m^2), emphasizing the urgency for erosion prevention and mitigation. When soil loss surpasses the T factor, the land no can longer sustain fertility until additional conservation measures are implemented.

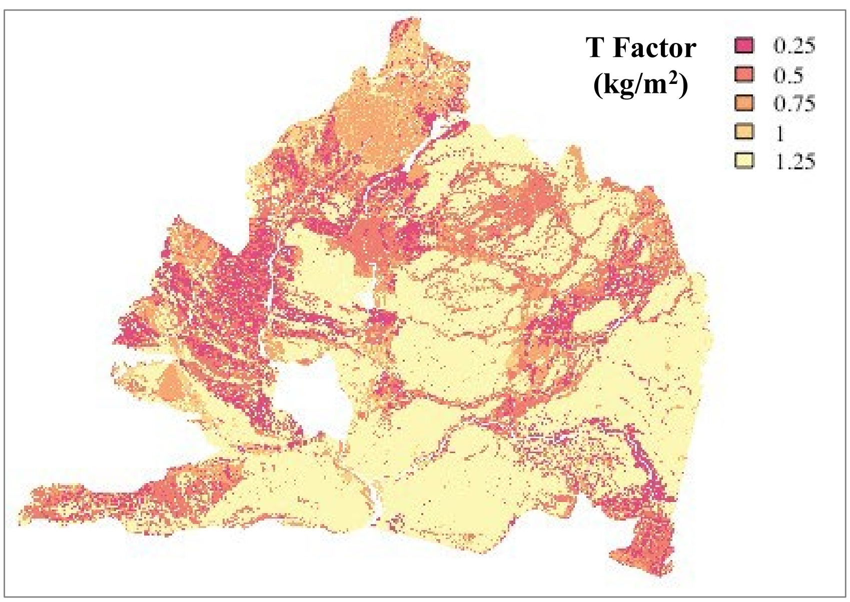

Figure 7. T Factor (kg/m^2/year) in the Columbia Plateau at 30-m spatial resolution

Errors and Assumptions

In my study, only WF and SLR_c included temporally dynamic inputs, whereas K_r, EF, and SCF were static. This increases the importance of correctly calculating WF and SLR_c and minimizing their simplification.

The distribution of monthly WF (Supplementary Figure 3) looks nearly identical to the distribution of monthly PSL (Supplementary Figure 1), suggesting that WF may have had a greater impact than SLR_c. The maximum WF that occurred in August (343,836 kg/m) appears to be an extreme outlier according to two other studies that reported their average annual WF. Borrelli et al. (2017) presented an average annual range of 0 to > 1,000 kg/m in their WF map legend. Pi et al. (2017) reported a minimum daily WF of 0.010 kg/m and a maximum of 2.780 kg/m. This suggests I made an error when calculating WF, which was indeed the most difficult input factor to compute. The temporal resolutions of the parameters to calculate SW, SD, and the wind part of the WF equation differed from one another. I processed each input factor using their given time scale then aggregated to their daily values, the aggregation depended on the parameter. For example, I added each 3-hour value of evapotranspiration and rainfall to get their daily sum and number of days when there was rainfall, which I then used to calculate monthly SW. I averaged 3-hourly SD (value of 0 if snow depth was ≥ 25.4 mm, or 1 if snow depth was < 25.4 mm) to get the monthly SD. The error likely occurred when calculating the wind factor, which involved many steps to calculate how many times wind speed exceeded the threshold, the number of wind speed observations, and the number of days in the period. Additionally, instead of calculating WF with monthly values of the input parameters, I should have calculated daily WF and then averaged to get the monthly value.

SLR_c has a spatial distribution that generally aligns with the vegetation coverage observed in the region (Supplementary Figure 5). As previously described in the Revised Wind Erosion Equation section, I used NDVI as a proxy for canopy cover in the SLR_c equation. This means I am using a measure of vegetation greenness or healthiness instead of how much live vegetation covers the soil surface. SLR_c was lowest when NDVI was highest as healthy or dense vegetation covered the soil surface and reduced erosion potential. NDVI was typically the highest, and SLR_c lowest, during the spring to early summer months (April through June). The extreme outliers of WF seemed to mask any influence SLR_c may have had on the PSL distribution. Therefore, it is difficult to understand how closely the peaks and skewness of each monthly histogram align between the SLR_c and PSL.

There also is opportunity to use additional datasets to incorporate other factors that were otherwise simplified or excluded in this study, such as estimating the impact of tillage operations on soil roughness and crop residue. Beeson et al. (2020) demonstrates a workflow to use Landsat imagery to calculate the Normalized Difference Tillage Index to estimate conservation tillage at the field level. Another area of improvement may be introducing a dynamic threshold wind velocity using the relationships between soil properties and threshold friction velocity, as demonstrated in Borrelli et al. (2017). The Agricultural Land Use dataset (WSDA, 2023) could be better utilized to understand how land use impacts soil loss estimates. Additionally, field length of each agricultural field could be extracted from this dataset and combined with topography to calculate x (distance to the upwind field edge), instead of using the somewhat arbitrary constant value of 150 m.

Limitations and Reflections

Availability of datasets with adequate temporal and spatial resolution was one of this study's primary challenges. Using the GEE platform, I could compute the RWEQ model over an entire year using datasets with resolutions as fine as one hour and 10-meters. However, this was only possible with the datasets available in the GEE catalog. GEE soil property datasets for my study area were coarse (250-meter resolution). Instead, I used R to extract and process soil data from the NRCS gSSURGO database with 30-meter resolution. Combining datasets with differing spatial and temporal resolutions was somewhat difficult to program in GEE, hence the probable errors when aggregating the weather and climate data. As I often reached memory limits using the large weather and climate datasets in computations, I realized how important programmatic and computational efficiency are, even when working in a cloud environment like GEE.

As discussed in the requirements for RS applications in erosion modeling, the accuracy of the model is limited to the quality of the datasets used to parameterize the model. My implementation of RWEQ was not able to account for land management parameters such as crop rotations, tillage operations, or crop growth stages.

It was a challenge to work through this project without field data for model estimate validation, and without additional published studies. These resources would have better helped identify the magnitude of error in my results, and the uncertainty each parameter contributed. Additionally, I was limited in statistical analyses with such a small sample size of one simulation of one year's worth of soil loss estimates, whereas more advanced implementations of erosion models use many simulations to measure uncertainty.

FUTURE WORK

The first step of improving my study is to resolve all errors and assumptions previously discussed. Then I will improve the JavaScript code for data extraction, processing, and analyses in GEE by increasing computational efficiency. I also will refactor the code to allow user input to vary the area and time period of interest. The workflow could then be run repeatedly with varying parameters, which would allow for a sensitivity analysis and mapping of the whole state. Including parameters to assess erosion for more years will result in a better understanding of longer-term seasonality and temporal variability. Similar to the Daily Erosion Project (Gelder et al., 2018), scripts will be hosted in a public repository to improve the reproducibility and transparency of the model, which will also help others build upon and improve it.

Field data related to erosion in the Columbia Plateau is numerous (Chung et al., 2011; Feng and Sharratt, 2009; G. Feng and Sharratt, 2007; Saxton et al., 1999; Sharratt and Schillinger, 2005). These published manuscripts should be better utilized in calibration and validation of future erosion models. Other studies have also used the Dust Storm Index, and other RS-derived indices to validate their erosion model performance. Future iterations of this model will include validation of high erosion potential with imagery of dust storms and comparisons with several other studies in the literature.

Modeling only wind erosion paints an incomplete picture. RWEQ estimates that no erosion occurs when the soil is sufficiently wet (generally, precipitation > evapotranspiration). However, RWEQ does not account for water erosion that occurs when too much precipitation can lead to runoff. For a complete understanding of soil erosion, both wind- and water-driven erosion must be modeled.

Broader Statewide Effort to Address Erosion

The future work described here will be leveraged to launch the next phase of a statewide strategy to measure and reduce erosion. An interactive mapping tool will highlight erosion ‘hotspots’ across the landscape, estimate daily erosion, and aid in the planning of conservation projects in later stages of the project. The tool also will be leveraged to educate and engage the public about erosion, its impacts, and its mitigation measures. Using a small sensor network to measure air quality and ground truth map estimates, we can then identify farms in geographic ‘hotspots’ and incentivize conservation practices that may prevent or mitigate erosion.

CONCLUSIONS

Through this study, I provided a proof of concept for improving the use of a wind-driven soil erosion model by using current publicly available GIS and RS data to generate monthly soil loss estimates in the Columbia Plateau. Predictions at the monthly scale provide insight into the temporal variability of erosion and its drivers, which scientists, land managers, and policymakers can leverage to guide their research and conservation efforts.

Additionally, I lay the groundwork for developing a web application to visualize wind erosion susceptibility. Unlike static model outputs presented in manuscripts, the web application would provide growers and decision-makers an accessible, practical, and relevant decision-support tool for monitoring and managing soil erosion.

REFERENCES

Ashley, W.S., Strader, S., Dziubla, D.C., Haberlie, A., 2015. Driving Blind: Weather-Related Vision Hazards and Fatal Motor Vehicle Crashes. Bulletin of the American Meteorological Society 96, 755–778. https://doi.org/10.1175/BAMS-D-14-00026.1

Batista, P.V.G., Davies, J., Silva, M.L.N., Quinton, J.N., 2019. On the evaluation of soil erosion models: Are we doing enough? Earth-Science Reviews 197, 102898. https://doi.org/10.1016/j.earscirev.2019.102898

Beaudette, D., Skovlin, J., Roecker, S., Brown, A., 2023. soilDB: Soil Database Interface.

Beaudoing, H., Rodell, M., NASA/GSFC/HSL, 2020. GLDAS Noah Land Surface Model L4 3 hourly 0.25 x 0.25 degree, Version 2.1. https://doi.org/10.5067/E7TYRXPJKWOQ

Beeson, P.C., Daughtry, C.S.T., Wallander, S.A., 2020. Estimates of Conservation Tillage Practices Using Landsat Archive. Remote Sensing 12. https://doi.org/10.3390/rs12162665

Borrelli, P., Lugato, E., Montanarella, L., Panagos, P., 2017. A New Assessment of Soil Loss Due to Wind Erosion in European Agricultural Soils Using a Quantitative Spatially Distributed Modelling Approach. Land Degradation & Development 28, 335–344. https://doi.org/10.1002/ldr.2588

Borrelli, P., Meusburger, K., Ballabio, C., Panagos, P., Alewell, C., 2018. Object-oriented soil erosion modelling: A possible paradigm shift from potential to actual risk assessments in agricultural environments. Land Degradation & Development 29, 1270–1281. https://doi.org/10.1002/ldr.2898

Chung, S., Esser, A., Jones, S.S., Kennedy, A.C., Koenig, R.T., Kok, H., Lamb, B.K., Machado, S., McGuire, A.M., Papendick, R.I., Petersen, P.J., Saxton, K.E., Schillinger, W.F., Sharratt, B.S., Young, D.L., Young, F.L., 2011. Columbia Plateau PM10 Project [WWW Document]. Washington State University. URL https://pnw-winderosion.wsu.edu/research-findings/

Crooks, J.L., Cascio, W.E., Percy, M.S., Reyes, J., Neas, L.M., Hilborn, E.D., 2016. The Association between Dust Storms and Daily Non-Accidental Mortality in the United States, 1993–2005. Environmental Health Perspectives 124, 1735–1743. https://doi.org/10.1289/EHP216

Davis, N., Badger, J., Hahmann, A.N., Hansen, B.O., Olsen, B.T., Mortensen, N.G., Heathfield, D., Onninen, M., Lizcano, G., Lacave, O., 2019. Global Wind Atlas v3. https://doi.org/10.11583/DTU.9420803.v1

Didan, K., 2021. MODIS/Terra Vegetation Indices 16-Day L3 Global 250m SIN Grid V061. https://doi.org/10.5067/MODIS/MOD13Q1.061

DNR, 2021. Geologic Provinces of Washington [WWW Document]. URL https://www.dnr.wa.gov/programs-and-services/geology/explore-popular-geology/geologic-provinces-washington (accessed 1.28.21).

Duniway, M.C., Pfennigwerth, A.A., Fick, S.E., Nauman, T.W., Belnap, J., Barger, N.N., 2019. Wind erosion and dust from US drylands: a review of causes, consequences, and solutions in a changing world. Ecosphere 10, e02650. https://doi.org/10.1002/ecs2.2650

El Jazouli, A., Barakat, A., Ghafiri, A., El Moutaki, S., Ettaqy, A., Khellouk, R., 2017. Soil erosion modeled with USLE, GIS, and remote sensing: a case study of Ikkour watershed in Middle Atlas (Morocco). Geoscience Letters 4, 25. https://doi.org/10.1186/s40562-017-0091-6

Elnashar, A., Zeng, H., Wu, B., Fenta, A.A., Nabil, M., Duerler, R., 2021. Soil erosion assessment in the Blue Nile Basin driven by a novel RUSLE-GEE framework. The Science of the total environment 793, 148466–148466.

Evans, R., Brazier, R., 2005. Evaluation of modelled spatially distributed predictions of soil erosion by water versus field-based assessments. Environmental Science & Policy 8, 493–501. https://doi.org/10.1016/j.envsci.2005.04.009

Feng, G., Sharratt, B., 2009. Evaluation of the SWEEP model during high winds on the Columbia Plateau. Earth Surf. Process. Landforms 34, 1461–1468. https://doi.org/10.1002/esp.1818

Feng, G., Sharratt, B., 2007. Validation of WEPS for soil and PM10 loss from agricultural fields within the Columbia Plateau of the United States. Earth Surface Processes and Landforms 32, 743–753. https://doi.org/10.1002/esp.1434

Feng, G, Sharratt, B., 2007. Scaling from field to region for wind erosion prediction using the Wind Erosion Prediction System and geographical information systems. Journal of Soil and Water Conservation 62, 321–328.

Fischer, F.K., Kistler, M., Brandhuber, R., Maier, H., Treisch, M., Auerswald, K., 2018. Validation of official erosion modelling based on high-resolution radar rain data by aerial photo erosion classification. Earth Surface Processes and Landforms 43, 187–194. https://doi.org/10.1002/esp.4216

Flanagan, D.C., Gilley, J.E., Franti, T.G., 2007. Water Erosion Prediction Project (WEPP): Development History, Model Capabilities, and Future Enhancements. Transactions of the ASABE 50, 1603–1612. https://doi.org/10.13031/2013.23968

Fryrear, D., Bilbro, J., Saleh, A., Schomberg, H., Stout, J., Zobeck, T., 2000. RWEQ: Improved wind erosion technology. Journal of soil and water conservation 55, 183–189.

Fryrear, D., Saleh, A., Bilbro, J., Schomberg, H., Stout, J., Zobeck, T., 1998. Revised Wind Erosion Equation (RWEQ). Wind Erosion and Water Conservation Research Unit, USDA-ARS, Southern Plains Area Cropping Systems Research Laboratory, Technical Bulletin 1.

Fryrear, D., Stout, J., Hagen, L., Vories, E., 1991. Wind Erosion: Field Measurement and Analysis. Transactions of the ASAE 34, 0155. https://doi.org/10.13031/2013.31638

Gao, J., Wagner, L.E., Fox, F., Chung, S.H., Vaughan, J.K., Lamb, B.K., 2013. SPATIAL APPLICATION OF WEPS FOR ESTIMATING WIND EROSION IN THE PACIFIC NORTHWEST. TRANSACTIONS OF THE ASABE 56, 613–624.

Gelder, B., Sklenar, T., James, D., Herzmann, D., Cruse, R., Gesch, K., Laflen, J., 2018. The Daily Erosion Project – daily estimates of water runoff, soil detachment, and erosion. Earth Surface Processes and Landforms 43, 1105–1117. https://doi.org/10.1002/esp.4286

Gorelick, N., Hancher, M., Dixon, M., Ilyushchenko, S., Thau, D., Moore, R., 2017. Google Earth Engine: Planetary-scale geospatial analysis for everyone. Remote Sensing of Environment. https://doi.org/10.1016/j.rse.2017.06.031

Hagen, L.J., 1991. A wind erosion prediction system to meet user needs. Journal of soil and water conservation 46, 106–111.

Hijmans, R.J., Bivand, R., Pebesma, E., Sumner, M.D., 2023. terra: Spatial Data Analysis.

Hills, K., Benedict, C., 2021. Washington Soil Health Roadmap. Washington State University.

Hu, Y., Tian, G., Mayer, A.L., He, R., 2015. Risk assessment of soil erosion by application of remote sensing and GIS in Yanshan Reservoir catchment, China. Natural Hazards 79, 277–289. https://doi.org/10.1007/s11069-015-1841-4

Jarrah, M., Mayel, S., Tatarko, J., Funk, R., Kuka, K., 2020. A review of wind erosion models: Data requirements, processes, and validity. CATENA 187, 104388. https://doi.org/10.1016/j.catena.2019.104388

Jetten, V., Govers, G., Hessel, R., 2003. Erosion models: quality of spatial predictions. Hydrological Processes 17, 887–900. https://doi.org/10.1002/hyp.1168

Joshi, J.R., 2021. Quantifying the impact of cropland wind erosion on air quality: A high-resolution modeling case study of an Arizona dust storm. Atmospheric Environment 263, 118658. https://doi.org/10.1016/j.atmosenv.2021.118658

Kjelgaard, J.F., Chandler, D.G., 2004. Evidence for direct suspension of loessial soils on the Columbia Plateau. Earth Surface Processes and Landforms 29, 221–236. https://doi.org/10.1002/esp.1028

Kumar, R., Deshmukh, B., Kumar, A., 2022. Using Google Earth Engine and GIS for basin scale soil erosion risk assessment: A case study of Chambal river basin, central India. Journal of Earth System Science 131, 228. https://doi.org/10.1007/s12040-022-01977-z

Lal, R., 1998. Soil Erosion Impact on Agronomic Productivity and Environment Quality. Critical Reviews in Plant Sciences 17, 319–464. https://doi.org/10.1080/07352689891304249

Lal, R., Moldenhauer, W.C., 1987. Effects of soil erosion on crop productivity. Critical Reviews in Plant Sciences 5, 303–367. https://doi.org/10.1080/07352688709382244

Mahmoodabadi, M., Cerdà, A., 2013. WEPP calibration for improved predictions of interrill erosion in semi-arid to arid environments. Geoderma 204–205, 75–83. https://doi.org/10.1016/j.geoderma.2013.04.013

McGowan, L.D., Bryan, J., 2023. googledrive: An Interface to Google Drive.

McGuire, A., 2011. Controlling Early Season Wind Erosion in Columbia Basin Potato Fields (No. WSU Extension Publication FS025E). Washington State University.

Montanarella, L., Pennock, D.J., McKenzie, N., Badraoui, M., Chude, V., Baptista, I., Mamo, T., Yemefack, M., Singh Aulakh, M., Yagi, K., Young Hong, S., Vijarnsorn, P., Zhang, G.-L., Arrouays, D., Black, H., Krasilnikov, P., Sobocká, J., Alegre, J., Henriquez, C.R., de Lourdes Mendonça-Santos, M., Taboada, M., Espinosa-Victoria, D., AlShankiti, A., AlaviPanah, S.K., Elsheikh, E.A.E.M., Hempel, J., Camps Arbestain, M., Nachtergaele, F., Vargas, R., 2016. World’s soils are under threat. SOIL 2, 79–82. https://doi.org/10.5194/soil-2-79-2016

Nearing, M.A., 2000. Evaluating soil erosion models using measured plot data: accounting for variability in the data. Earth Surface Processes and Landforms 25, 1035–1043. https://doi.org/10.1002/1096-9837(200008)25:9<1035::AID-ESP121>3.0.CO;2-B

Panagos, P., Borrelli, P., Poesen, J., Ballabio, C., Lugato, E., Meusburger, K., Montanarella, L., Alewell, C., 2015. The new assessment of soil loss by water erosion in Europe. Environmental Science & Policy 54, 438–447. https://doi.org/10.1016/j.envsci.2015.08.012

Pandey, A., Chowdary, V.M., Mal, B.C., 2007. Identification of critical erosion prone areas in the small agricultural watershed using USLE, GIS and remote sensing. Water Resources Management 21, 729–746. https://doi.org/10.1007/s11269-006-9061-z

Pi, H., Huggins, D.R., Abatzoglou, J.T., Sharratt, B., 2020. Modeling Soil Wind Erosion From Agroecological Classes of the Pacific Northwest in Response to Current Climate. Journal of Geophysical Research: Atmospheres 125, e2019JD031104. https://doi.org/10.1029/2019JD031104

Pi, H., Sharratt, B., Feng, G., Lei, J., 2017. Evaluation of two empirical wind erosion models in arid and semi-arid regions of China and the USA. Environ. Model. Softw. 91, 28–46. https://doi.org/j.envsoft.2017.01.013

Pimentel, D., 2006. Soil Erosion: A Food and Environmental Threat. Environ Dev Sustain 8, 119–137. https://doi.org/10.1007/s10668-005-1262-8

Pimentel, D., Harvey, C., Resosudarmo, P., Sinclair, K., et al, 1995. Environmental and economic costs of soil erosion and conservation benefits. Science 267, 1117.

Poesen, J., 2018. Soil erosion in the Anthropocene: Research needs. Earth Surface Processes and Landforms 43, 64–84. https://doi.org/10.1002/esp.4250

Polykretis, C., Alexakis, D.D., Grillakis, M.G., Manoudakis, S., 2020. Assessment of Intra-Annual and Inter-Annual Variabilities of Soil Erosion in Crete Island (Greece) by Incorporating the Dynamic "Nature" of R and C-Factors in RUSLE Modeling. Remote Sensing 12. https://doi.org/10.3390/rs12152439

Pondeca, M.S.F.V.D., Manikin, G.S., DiMego, G., Benjamin, S.G., Parrish, D.F., Purser, R.J., Wu, W.-S., Horel, J.D., Myrick, D.T., Lin, Y., Aune, R.M., Keyser, D., Colman, B., Mann, G., Vavra, J., 2011. The Real-Time Mesoscale Analysis at NOAA's National Centers for Environmental Prediction: Current Status and Development. Weather and Forecasting 26, 593–612. https://doi.org/10.1175/WAF-D-10-05037.1

R Core Team, 2023. R: A Language and Environment for Statistical Computing. R Foundation for Statistical Computing, Vienna, Austria.

Renard, K.G., Foster, G.R., Weesies, G.A., McCool, D.K., Yoder, D.C., 1996. Predicting soil erosion by water: A guide to conservation planning with the Revised Universal Soil Loss Equation (RUSLE). Agriculture handbook 703.

Rickson, R.J., 2014. Can control of soil erosion mitigate water pollution by sediments? Science of The Total Environment 468–469, 1187–1197. https://doi.org/10.1016/j.scitotenv.2013.05.057

Saxton, K., Chandler, D., Schillinger, W., 1999. Wind Erosion and Air Quality Research in the Northwest U.S. Columbia Plateau: Organization and Progress, in: Sustaining the Global Farm, Selected Papers From the 10th International Soil Conservation Organization Meeting. Presented at the Int. Soil Conserv. Organ., West Lafayette, Indiana.

Schertz, D.L., Nearing, M., 2006. Erosion tolerance/soil loss tolerance. Encyclopedia of Soil Science 640–642.

Schillinger, W.F., Papendick, R.I., 2008. Then and Now: 125 Years of Dryland Wheat Farming in the Inland Pacific Northwest. Agronomy Journal 100, S-166-S-182. https://doi.org/10.2134/agronj2007.0027c

Sharratt, B.S., Schillinger, W.F., 2005. The Columbia Plateau Wind Erosion/ Air Quality Project: Predicting and Controlling Windblown Dust. Presented at the American Meteorological Society.

Sharratt, B.S., Tatarko, J., Abatzoglou, J.T., Fox, F.A., Huggins, D., 2015. Implications of climate change on wind erosion of agricultural lands in the Columbia plateau. Weather and Climate Extremes 10, 20–31. https://doi.org/10.1016/j.wace.2015.06.001

Shirriff, K., KC, K.B., Berg, A., 2022. Exploring the Relationship between Cover Crop Adoption and Soil Erosion Severity: A Case Study from the Simcoe Watershed, Ontario, Canada. Land 11. https://doi.org/10.3390/land11070988

Skidmore, E.L., Tatarko, J., 1990. Stochastic wind simulation for erosion modeling. Transactions of the ASAE 33, 1893–1899.

Soil Survey Staff, 2023. Gridded Soil Survey Geographic (gSSURGO) Database for Washington State United States Department of Agriculture, Natural Resources Conservation Service. https://gdg.sc.egov.usda.gov/

Stroosnijder, L., 2005. Measurement of erosion: Is it possible? CATENA 64, 162–173. https://doi.org/10.1016/j.catena.2005.08.004

Tatarko, J., Wagner, L., Fox, F., 2019. The wind erosion prediction system and its use in conservation planning. Bridging among disciplines by synthesizing soil and plant processes 8, 71–101.

Trout, T.J., Johnson, L.F., Gartung, J., 2008. Remote Sensing of Canopy Cover in Horticultural Crops. HortScience 43, 333–337. https://doi.org/10.21273/HORTSCI.43.2.333

Uri, N.D., 2000. Agriculture and the Environment – The Problem of Soil Erosion. Journal of Sustainable Agriculture 16, 71–94. https://doi.org/10.1300/J064v16n04_07

USGS, 2020. 3D Elevation Program 10-Meter Resolution Digital Elevation Model. U.S. Geological Survey.

Vaughn, K., 2022. It’s dust storm season [WWW Document]. Washington Department of Ecology. URL https://ecology.wa.gov/Blog/Posts/March-2022/It-s-Dust-Storm-Season (accessed 7.13.23).

Vrieling, A., 2006. Satellite remote sensing for water erosion assessment: A review. CATENA 65, 2–18. https://doi.org/10.1016/j.catena.2005.10.005

Wagner, L.E., 2013. A history of Wind Erosion Prediction Models in the United States Department of Agriculture: The Wind Erosion Prediction System (WEPS). Aeolian Research 10, 9–24. https://doi.org/10.1016/j.aeolia.2012.10.001

Wang, W., Samat, A., Ge, Y., Ma, L., Tuheti, A., Zou, S., Abuduwaili, J., 2020. Quantitative Soil Wind Erosion Potential Mapping for Central Asia Using the Google Earth Engine Platform. Remote Sensing 12. https://doi.org/10.3390/rs12203430

Watson, C., 2022. Many researchers say they'll share data — but don't. Nature 606, 853–853. https://doi.org/10.1038/d41586-022-01692-1

Wickham, H., François, R., Henry, L., Müller, K., Vaughan, D., 2023. dplyr: A Grammar of Data Manipulation.

Wilkinson, M.D., Dumontier, M., Aalbersberg, Ij.J., Appleton, G., Axton, M., Baak, A., Blomberg, N., Boiten, J.-W., da Silva Santos, L.B., Bourne, P.E., Bouwman, J., Brookes, A.J., Clark, T., Crosas, M., Dillo, I., Dumon, O., Edmunds, S., Evelo, C.T., Finkers, R., Gonzalez-Beltran, A., Gray, A.J.G., Groth, P., Goble, C., Grethe, J.S., Heringa, J., 't Hoen, P.A.C., Hooft, R., Kuhn, T., Kok, R., Kok, J., Lusher, S.J., Martone, M.E., Mons, A., Packer, A.L., Persson, B., Rocca-Serra, P., Roos, M., van Schaik, R., Sansone, S.-A., Schultes, E., Sengstag, T., Slater, T., Strawn, G., Swertz, M.A., Thompson, M., van der Lei, J., van Mulligen, E., Velterop, J., Waagmeester, A., Wittenburg, P., Wolstencroft, K., Zhao, J., Mons, B., 2016. The FAIR Guiding Principles for scientific data management and stewardship. Sci Data 3, 160018. https://doi.org/10.1038/sdata.2016.18

Woodruff, N.P., Siddoway, F.H., 1965. A wind erosion equation. Soil Science Society of America Journal 29, 602–608.

WSDA, 2023. Agricultural Land Use. Natural Resource Assessment Section, Washington State Department of Agriculture.

WSDA, 2021. Agriculture in the Columbia Basin (No. AGR PUB 101-885). Washington State Department of Agriculture, Olympia, WA.

WSU, 2023. AgWeatherNet. Washington State University. https://weather.wsu.edu/

Yang, G., Sun, R., Jing, Y., Xiong, M., Li, J., Chen, L., 2022. Global assessment of wind erosion based on a spatially distributed RWEQ model. Progress in Physical Geography: Earth and Environment 46, 28–42. https://doi.org/10.1177/03091333211030608

Zhang, M., Viscarra Rossel, R.A., Zhu, Q., Leys, J., Gray, J.M., Yu, Q., Yang, X., 2022. Dynamic Modelling of Water and Wind Erosion in Australia over the Past Two Decades. Remote Sensing 14. https://doi.org/10.3390/rs14215437

Zobeck, T.M., Parker, N.C., Haskell, S., Guoding, K., 2000. Scaling up from field to region for wind erosion prediction using a field-scale wind erosion model and GIS. Agriculture, ecosystems & environment 82, 247–259.

SUPPLEMENTARY MATERIALS

Supplementary Table 1. Overview of wind erosion models implemented in the Columbia Plateau PM10 Project, adapted from (Jarrah et al., 2020).

Model	Type	Primary Input Parameters	Output	Columbia Plateau Implementations
Revised Wind Equation (RWEQ) (Fryrear et al., 1998)	Empirical/ process-based	**Erodible fraction** (aggregates > 0.84 mm); **Soil crust** (% clay and organic matter); **Soil wetness** (rainfall, irrigation, solar radiation); **Weather** (wind velocity, wind direction, rainfall, solar radiation, air temperature, snowfall); **Tillage** (soil roughness); **Field geometry** (field size, shape, orientation, length); **Crop** (live canopy cover, residue height, stalk diameter, number); **Hills** (slope gradient, length)	Average soil loss per area per year or shorter period	(Pi et al., 2017)
Wind Erosion Prediction System (WEPS) (Hagen, 1991)	Process-based	**Soil erodibility** (% sand, silt, clay, bulk density, soil layer thickness), **Surface cover** (rocks); **Soil surface condition** (random and oriented roughness, aggregate size distribution, surface moisture); **Climate** (wind velocity, wind direction); **Management** (tillage and crop operations)	Soil loss/deposition by direction and size class as saltation plus creep, suspension and PM_{10}	(G. Feng and Sharratt, 2007; G Feng and Sharratt, 2007; Pi et al., 2020)

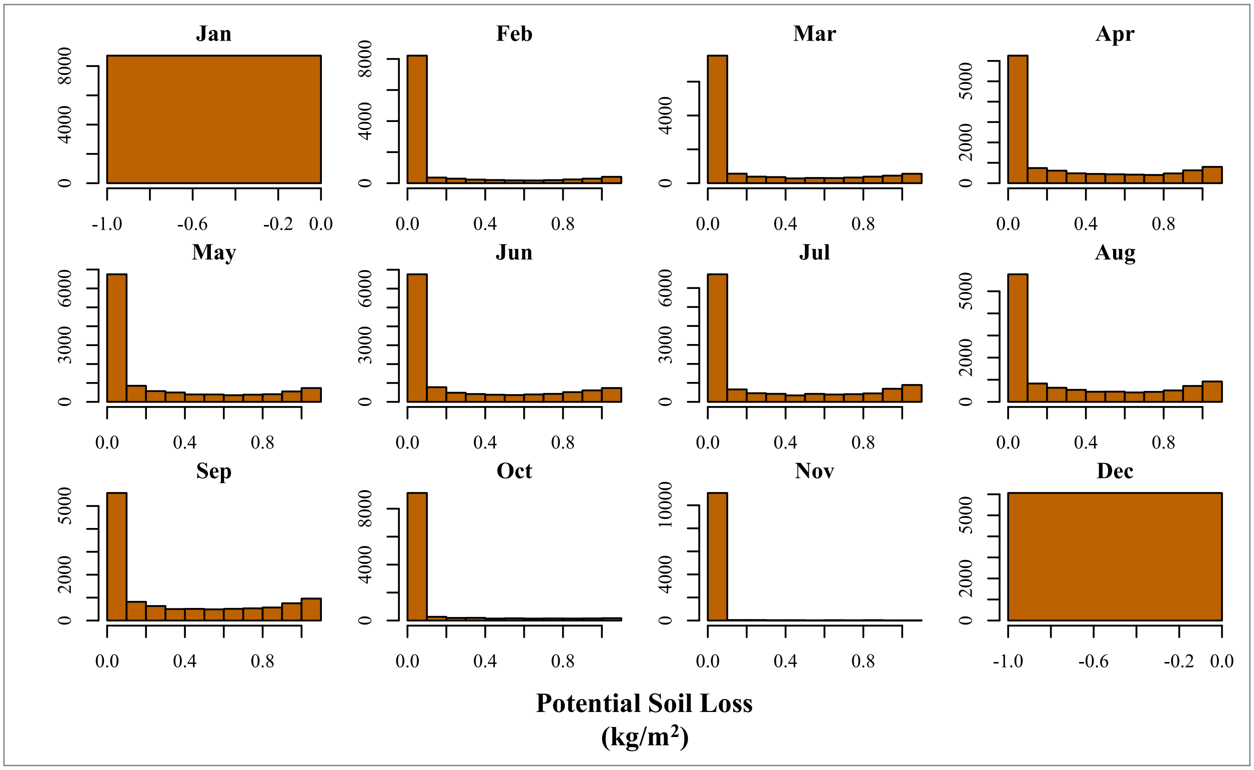

Supplementary Figure 1. Monthly histograms of wind-driven PSL (kg/m^2) across all pixels in the Columbia Plateau study area in 2018

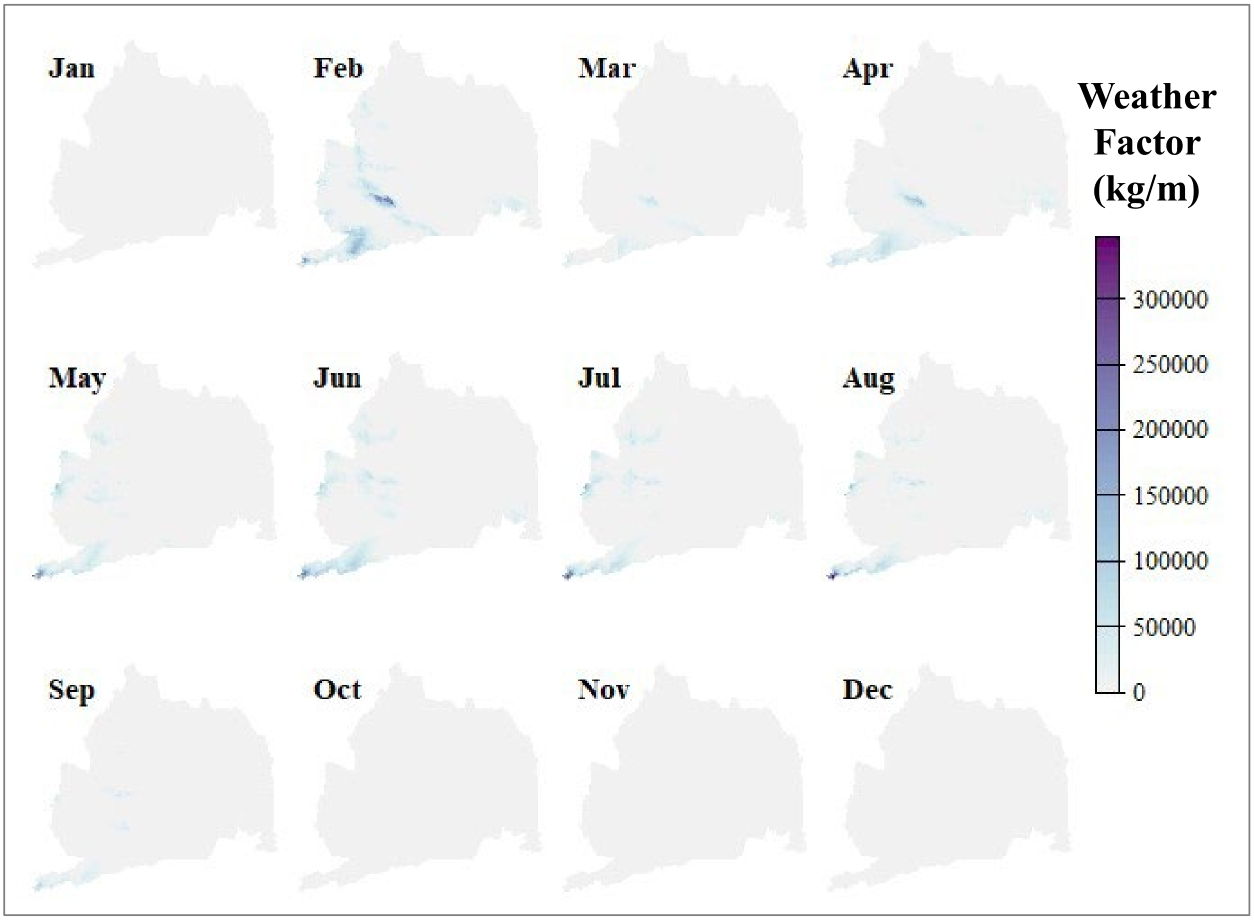

Supplementary Figure 2. Monthly WF (kg/m) for 2018 at 0.25° spatial resolution

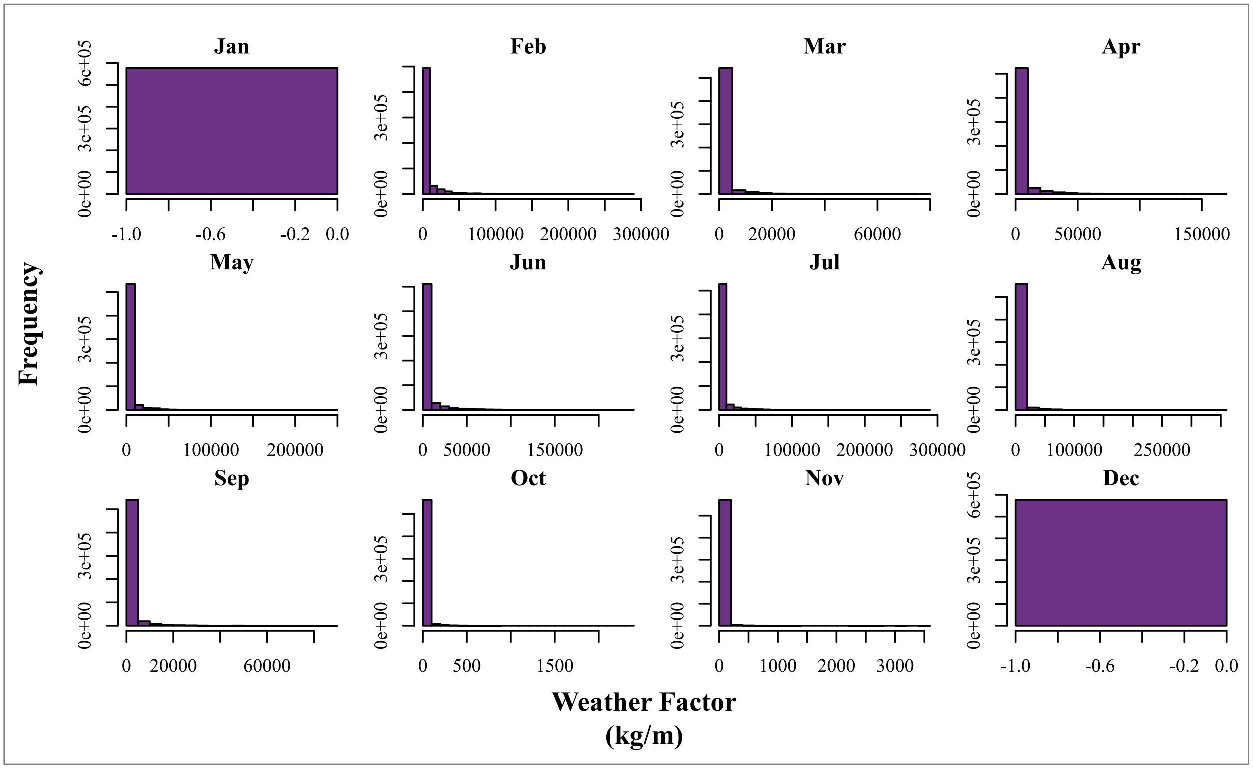

Supplementary Figure 3. Monthly histograms of WF (kg/m) across all pixels in the Columbia Plateau study area in 2018

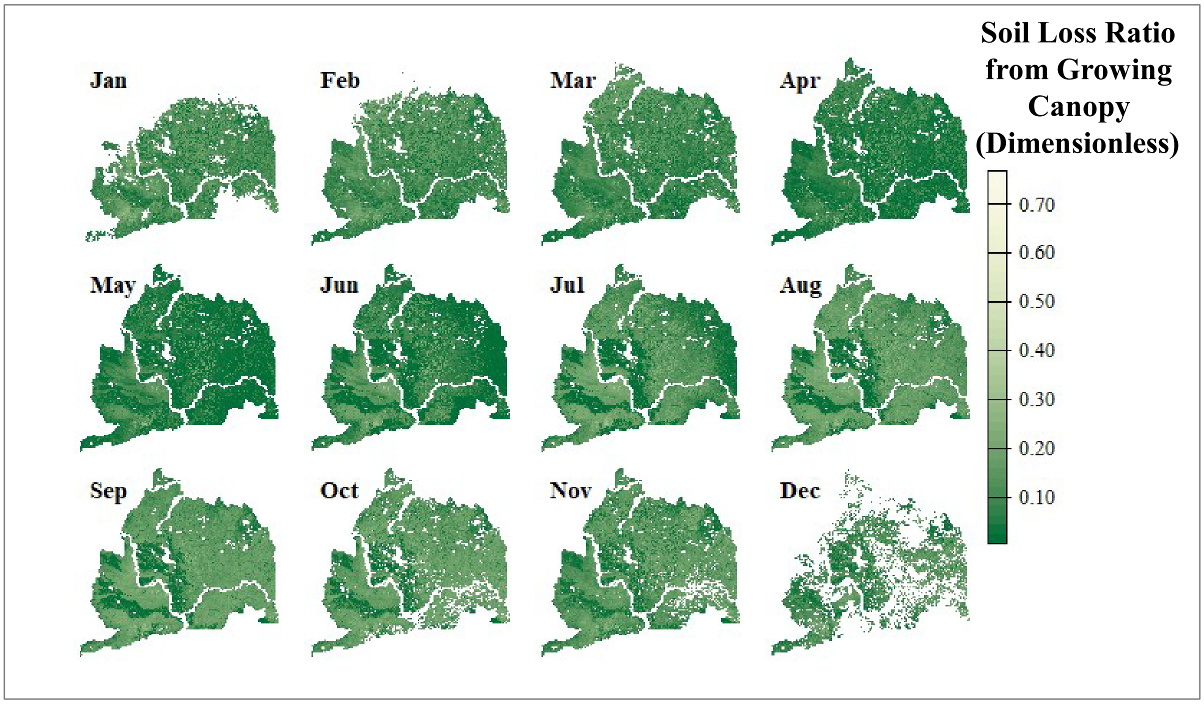

Supplementary Figure 4. Monthly Soil Loss Ratio from Growing Canopy Factor for 2018 was calculated using NDVI as a proxy for canopy cover at 250-m spatial resolution. Poor quality and non-land pixels (as determined by MOD13Q1 quality assurance band and bitmask) are masked.

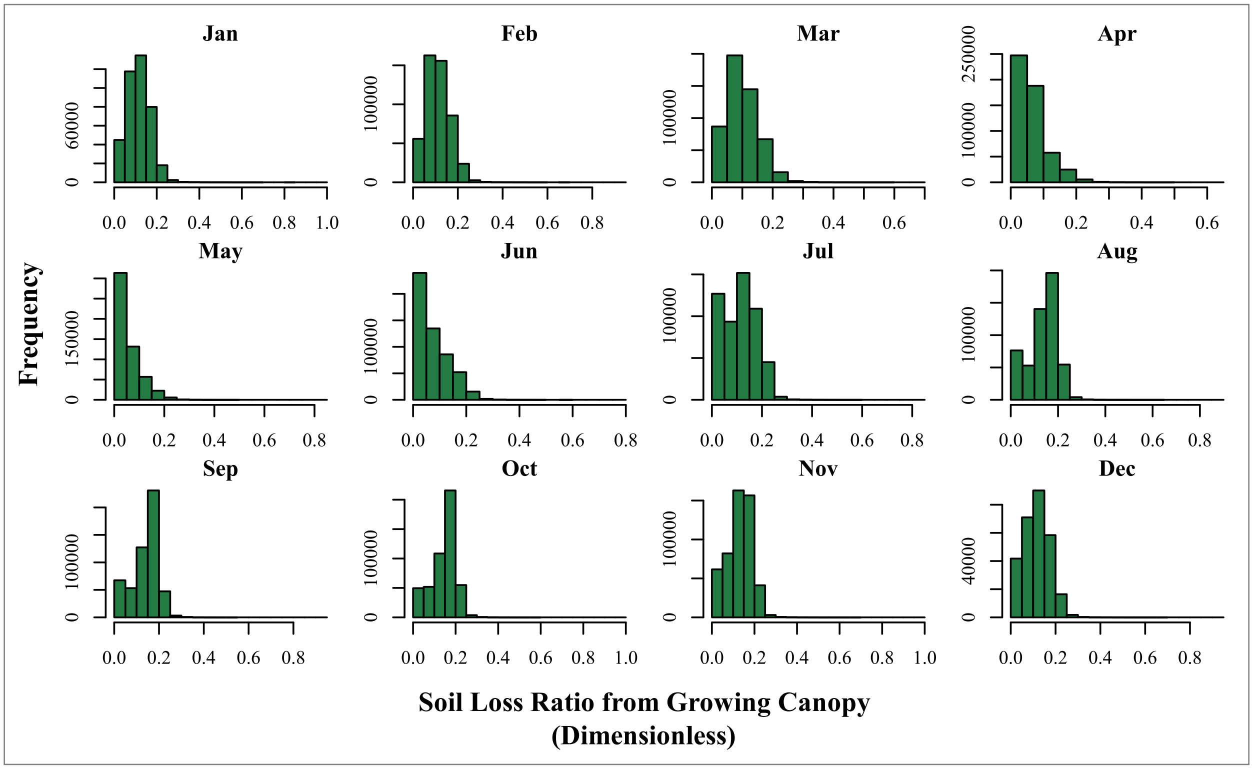

Supplementary Figure 5. Monthly histograms of SLR_c across all pixels in the Columbia Plateau study area in 2018

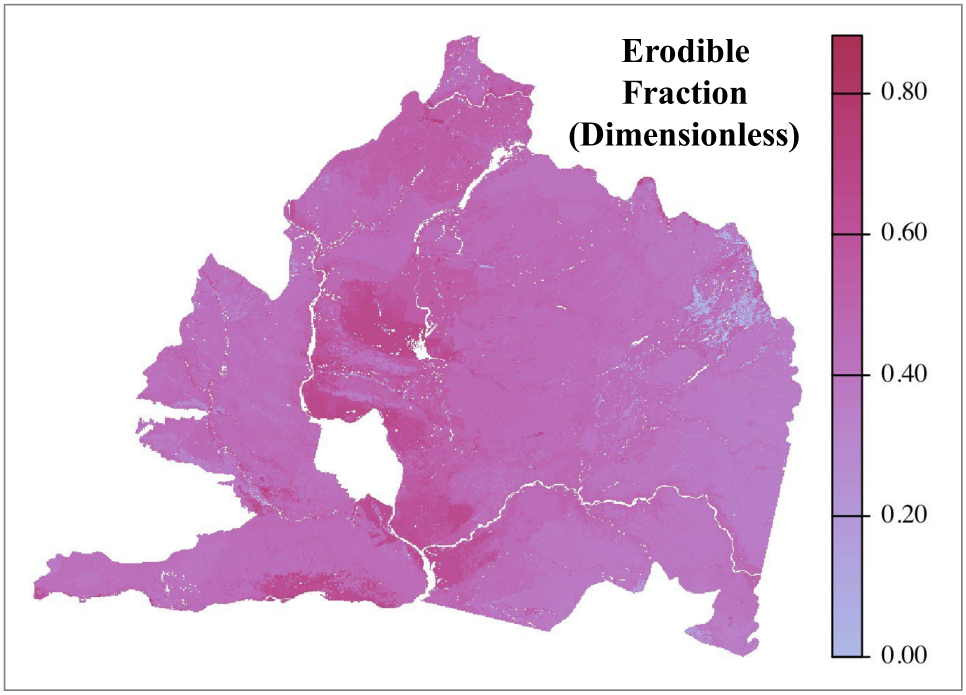

Supplementary Figure 6. EF at 30-m spatial resolution

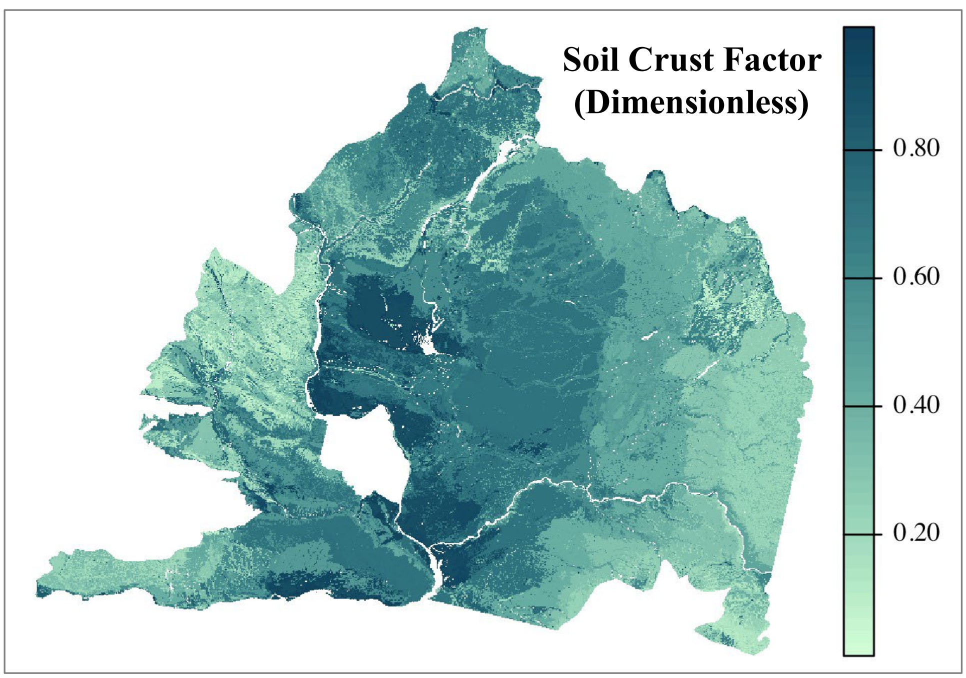

Supplementary Figure 7. SCF at 30-m spatial resolution

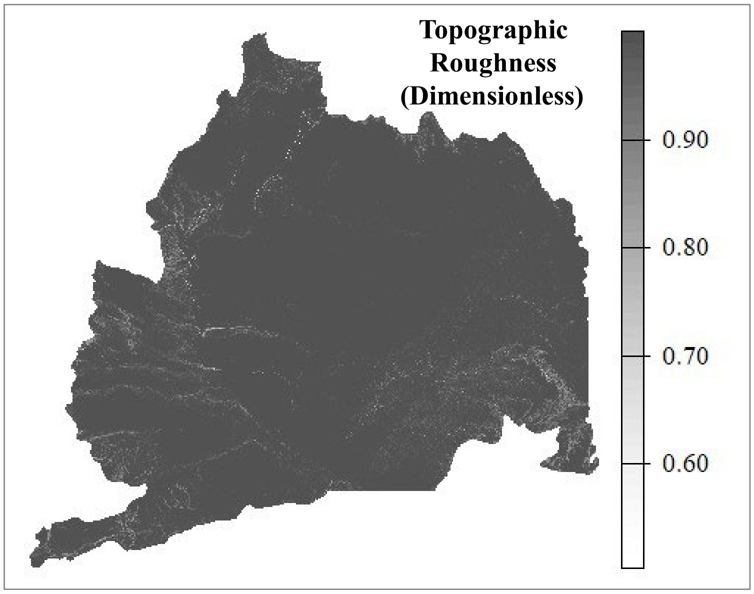

Supplementary Figure 8. K_r at 10-m spatial resolution